JPET Fast Forward. Published on January 23, 2015 as DOI: 10.1124/jpet.114.221523
This article has not been copyedited and formatted. The final version may differ from this version.

Species-specific Influence of Lithium on the Activity of SLC13A5 (NaCT): Lithium-induced Activation is Specific for the Transporter in Primates

Elangovan Gopal, Ellappan Babu, Sabarish Ramachandran, Yangzom D. Bhutia, Puttur D. Prasad, and Vadivel Ganapathy

Department of Cell Biology and Biochemistry, Texas Tech University Health Sciences Center, Lubbock, TX 79430 (E.B., S.R., Y.D.B., V.G); Department of Biochemistry and Molecular Biology, Medical College of Georgia, Georgia Regents University, Augusta, GA 30912 (E.G., P.D.P).

Running Title: Activation of SLC13A5 by lithium is unique to primates

Corresponding author: Vadivel Ganapathy, Department of Cell Biology and Biochemistry, Texas Tech University Health Sciences Center, Lubbock, TX 79430. Tel.: 806-743-2518; Fax: 806-743-2990; email: vadivel.ganapathy@ttuhsc.edu

Text pages: 33

Tables: 1

Figures: 9

References: 26

Words in Abstract: 250

Words in Introduction: 673

Words in Discussion: 1952

ABBREVIATIONS: NaCT, Na^+-coupled citrate transporter; SLC, solute carrier; IC_{50}, concentration necessary to cause 50% inhibition; ED_{50}, concentration necessary to cause 50% maximal effect; HRPE, human retinal pigment epithelial

Recommended section assignment: Cellular and Molecular

JPET Fast Forward. Published on January 23, 2015 as DOI: 10.1124/jpet.114.221523
This article has not been copyedited and formatted. The final version may differ from this version.

ABSTRACT

NaCT (SLC13A5) is a Na^+-coupled transporter for Krebs cycle intermediates; it is expressed predominantly in the liver. Human NaCT is relatively specific for citrate compared to other Krebs cycle intermediates. The transport activity of human NaCT is stimulated by Li^+ whereas that of rat NaCT is inhibited by Li^+. Here we studied the influence of Li^+ on NaCTs cloned from eight different species. Li^+ stimulated the activity of only NaCTs from primates (human, chimpanzee and monkey); in contrast, NaCTs from non-primate species (mouse, rat, dog, and zebrafish) were inhibited by Li^+. *C. elegans* NaCT was not affected by Li^+. With human NaCT, the Li^+-induced increase in transport activity was associated with the conversion of the transporter from a low-affinity/high-capacity type to a high-affinity/low-capacity type. H^+ was able to substitute for Li^+ in eliciting the stimulatory effect. The amino acid phenylalanine at position 500 in human NaCT was critical for Li^+/H^+-induced stimuation. Mutation of this amino acid to tryptophan (F500W) markedly increased the basal transport activity of human NaCT in the absence of Li^+, but the ability of Li^+ to stimulate the transporter was almost completely lost with this mutant. Substitution of Phe-500 with tryptophan in human NaCT converted the transporter from a low-affinity/high-capacity type to a high-affinity/low-capacity type, an effect similar to that of Li^+ on the wild type NaCT. These studies show that Li^+-induced activation of NaCT is specific for the transporter in primates and that the region surrounding Phe-500 in primate NaCTs is important for the Li^+ effect.

JPET Fast Forward. Published on January 23, 2015 as DOI: 10.1124/jpet.114.221523
This article has not been copyedited and formatted. The final version may differ from this version.

Introduction

We have recently cloned and functionally characterized a Na^+-coupled transporter for citrate and other intermediates of Krebs cycle from rat, human, mouse and *C. elegans* and named the transporter NaCT (Na^+-coupled Citrate Transporter) (Inoue et al., 2002a,b; 2004; Fei et al., 2004). NaCT is identified as SLC13A5 according to the Human Genome Organization nomenclature (Markovich and Murer, 2004; Pajor, 2006). In humans, SLC13A5 mRNA is expressed abundantly in the liver, and to a much lesser extent in the brain and testes (Inoue et al., 2002b). In the rat however, the transporter mRNA is expressed in the liver and testes with comparable abundance, and at relatively much lower levels in the brain (Inoue et al., 2002a). There are also important differences in substrate selectivity between human and rodent NaCTs. While the rat and mouse NaCTs recognize citrate with high affinity (K_t: rat, ~20 μM; mouse, ~40 μM), these transporters also interact with succinate with appreciable affinity (K_t: rat, ~170 μM; mouse, ~40 μM) (Inoue et al., 2002a; 2004). In contrast, human NaCT exhibits relatively lower affinity for citrate (K_t, ~600 μM) but is relatively more selective for citrate (Inoue et al., 2002b). Based on substrate specificity, NaCT is the mammalian functional ortholog of Indy (I am not dead yet) in *Drosophila* (Rogina et al., 2000) even though the mammalian NaCT is Na^+-dependent whereas the *Drosophila* Indy is Na^+-independent (Knauf et al., 2002, 2006; Inoue et al., 2002c). Among the various Krebs cycle intermediates, citrate is present at highest concentration in circulation in humans (~160 μM). In the liver where NaCT is expressed abundantly and is present specifically in the sinusoidal membrane (Gopal et al., 2007), the transporter mediates Na^+-coupled concentrative uptake of citrate from blood into hepatocytes for subsequent utilization in metabolism (Inoue et al., 2003). Citrate entering into the cytoplasm of the hepatocytes via NaCT is avidly used for the synthesis of fatty acids (Inoue et al., 2003;

JPET Fast Forward. Published on January 23, 2015 as DOI: 10.1124/jpet.114.221523
This article has not been copyedited and formatted. The final version may differ from this version.

Ganapathy and Fei, 2005). As such, deletion of the transporter in mice protects against diet-induced insulin resistance and metabolic syndrome (Birkenfeld et al., 2011). In the testes, NaCT is expressed in sperm cells (unpublished data). Since seminal fluid contains high concentrations of citrate (~130 mM) (Kline et al., 2006), we speculate that NaCT in spermatozoa mediates the concentrative uptake of citrate from seminal fluid into sperm cells to serve as a metabolic fuel. In the brain, NaCT is expressed specifically in neuronal cells (Wada et al., 2006; Yodoya et al., 2006) where the most likely function of the transporter is to transport citrate from extracellular medium for subsequent utilization in metabolism for ATP production.

The differences between human NaCT and rodent NaCTs in substrate selectivity, substrate affinity, and tissue expression pattern are relatively less pronounced compared to the difference in the influence of lithium on these transporters. The Na^+-coupled transport of citrate via rodent NaCTs is inhibited by Li^+ with an IC_{50} of ~2 mM whereas the Na^+-coupled transport of citrate via human NaCT is stimulated by Li^+ with an ED_{50} of ~2 mM (Inoue et al., 2003). The stimulation of human NaCT by Li^+ is associated with a marked increase in substrate affinity (Inoue et al., 2003). We found this finding very interesting. Treatment with lithium in humans for affective disorders is associated with significant weight gain and increased circulating levels of triglycerides (Bergmann et al., 2007; Bardini et al., 2009). Since NaCT mediates concentrative uptake of citrate from the circulation into hepatocytes for subsequent utilization in cholesterol and fatty acid synthesis, we speculated that stimulation of NaCT-mediated delivery of citrate into hepatocytes for subsequent utilization for fat synthesis contributes to the weight gain associated with lithium therapy (Inoue et al., 2003; Ganapathy and Fei, 2005). These findings suggest that the stimulation of human NaCT by Li^+ may have important clinical implications. In the present study, we explored further the species-specific influence of Li^+ on the function of NaCT by

JPET Fast Forward. Published on January 23, 2015 as DOI: 10.1124/jpet.114.221523
This article has not been copyedited and formatted. The final version may differ from this version.

studying the effects of Li^+ on NaCTs cloned from two non-human primates (monkey and chimpanzee) and from two additional non-primate species (dog and zebrafish).

Methods

Materials. [^{14}C]-Citrate (specific radioactivity, 55 mCi/mmol) was purchased from Moravek Biochemicals (Brea, CA). Unlabeled lactate, succinate, malate, α-ketoglutarate, and citrate were purchased from Sigma Aldrich (St. Louis, MO). Total RNA samples from dog liver, monkey (Rhesus) liver, and chimpanzee liver were used in RT-PCR to prepare full-length NaCT cDNAs from the respective species. The cDNAs for NaCTs from rat, mouse, human, and *C. elegans* have been described in our earlier publications (Inoue et al., 2002a,b; 2004; Fei et al., 2004).

Female frogs (*Xenopus laevis*), used as the source of oocytes for heterologous expression of cloned NaCTs, were purchased from Xenopus 1, Inc. (Dexter, MI). The protocol for the use of frogs in these studies was approved by the institutional Animal Care and Use Committee.

Cloning of monkey, chimpanzee, dog, and zebrafish NaCT cDNAs. Monkey and chimpanzee NaCT cDNAs were cloned by RT-PCR using liver RNA samples from the respective species as the template. The following primers were used for both species: 5'-ATATATACCCTCCCGCGCGATG-3' (forward) and 5'-GTCTAGACTAAGTCTCAATATGTG-3' (reverse). The forward primer contained the start codon ATG at its 3'-end and an *Eco*RI site at its 5'-end. The reverse primer contained the coding sequence for the last 5 amino acids (Thr-His-Ile-Glu-Thr) of the carboxy terminus of human NaCT at its 3'-end and an *Xba*I site at its 5'-end. The restriction sites were added for subcloning the PCR products into pcDNA vector. The PCR products were first subcloned into pGEM-T Easy vector and the cDNA insert was released from the construct by *Eco*RI/*Xba*I digestion for

subcloning into pcDNA vector following its linearization with *EcoR*I/*Xba*I. Both strands of the cDNAs were sequenced and the amino acid sequences of monkey and chimpanzee NaCTs elucidated. Dog (*Canis lupus familiaris*) NaCT cDNA sequence is available in the GenBank (accession no. XM_843480); RT-PCR primers for cloning dog NaCT cDNA were designed based on this nucleotide sequence: 5'-GATATATAGCCATGGCCTCGGCGCTCAGCTA-3' (forward) and 5'-GCGTCTAGACTAGGTCTCGATATTCGTCACG-3' (reverse). The PCR product was cloned into pcDNA as described above for primate NaCTs. Both strands of the cDNAs were sequenced. The deduced amino sequence of the cloned dog NaCT was identical to the sequence reported in the GenBank. The zebrafish NaCT cDNA was isolated from a zebrafish cDNA library constructed in pSPORT1 vector (Kozlowski et al., 2008). A ~1.4 kbp fragment of the rat NaCT cDNA was used as the probe to screen the library. Both strands of the full-length clone were sequenced.

Site-directed mutagenesis. The codon-500 in human NaCT cDNA encodes phenylalanine. This codon was changed by site-directed mutagenesis to code for tyrosine (F500Y), tryptophan (F500W), alanine (F500A), valine (F500V), isoleucine (F500I), leucine (F500L), methionine (F500M), aspartate (F500D), and lysine (F500K). The QuickChange site-directed mutagenesis kit (Stratagene) was used to generate the mutants according to the manufacturer's protocol, and the details of the procedure have been described previously (Wu et al., 1999). The entire coding region of the mutant cDNAs was sequenced to confirm the presence of the introduced mutations.

Functional expression of NaCT cDNAs in a mammalian cell line. The human retinal pigment epithelial cell line HRPE was used for heterologous expression of the cloned NaCT cDNAs. The vaccinia virus expression technique was employed for this purpose, and the details of the procedure have been published previously (Inoue et al., 2002a,b; 2004). The activity of

NaCT was monitored by measuring [^{14}C]-citrate uptake. Uptake measurements were performed at 37 ^{o}C in a NaCl-containing buffer, pH 7.5 (composition: 25 mM Hepes/Tris buffer, 140 mM NaCl, 5.4 mM KCl, 1.8 mM $CaCl_2$, 0.8 mM $MgSO_4$, and 5 mM glucose). The uptake of citrate in control cells transfected with vector alone was very low, and the uptake increased in NaCT cDNA-transfected cells by a minimum of 25-fold. With each of the NaCTs studied here, the cDNA-specific citrate uptake was linear at least up to 45 min. In experiments in which the cation dependence of NaCT activity was studied, NaCl in the uptake buffer was replaced isoosmotically with LiCl, KCl or *N*-methyl-D-glucamine (NMDG) chloride. To investigate the dependence of NaCT activity on Cl^-, NaCl in the uptake buffer was replaced isoosmotically with sodium gluconate; in addition, KCl was replaced with potassium gluconate, and $CaCl_2$ with calcium gluconate. The kinetic parameters Michaelis constant (K_t) and maximal velocity (V_{max}) were determined from saturation kinetics of citrate uptake. To investigate the influence of Li^+ on NaCT activity, citrate uptake was measured in the presence of NaCl with varying concentrations of LiCl; equimolar concentrations of NMDG chloride were added for controls to adjust for osmolality.

Functional expression of rat and human NaCTs in *Xenopus laevis* oocytes. Capped cRNA was prepared from the cloned rat or human NaCT cDNAs using the mMESSAGE mMACHINE kit (Ambion, Austin, TX). Functional expression in *X. laevis* oocytes was carried out as described previously (Inoue et al., 2004) by microinjection of cRNA (50 ng/oocyte) into mature oocytes. Uninjected oocytes were used as negative controls. Electrophysiological studies were performed 4-6 days after cRNA injection using the two-microelectrode voltage-clamp technique. Oocytes were perifused with a NaCl-containing buffer (100 mM NaCl, 2 mM KCl, 1 mM $MgCl_2$, 1 mM $CaCl_2$, 3 mM Hepes, 3 mM Mes, and 3 mM Tris, pH 7.5), followed by the

same buffer containing citrate. The membrane potential was clamped at – 50 mV. The currents measured in the absence of citrate were subtracted from the currents measured in the presence of citrate to calculate citrate-specific currents. In uninjected oocytes, the citrate-specific currents were undetectable. The citrate-induced currents in NaCT-expressing oocytes were taken as a measure of NaCT activity. The stimulation of NaCT activity by Li^+ was studied by analyzing the citrate-induced currents in the NaCl-containing buffer with varying concentrations of LiCl; equimolar concentrations of NMDG chloride were added to the buffer to adjust for osmolality. The kinetic parameters K_t and V_{max} were determined from the saturation kinetics of citrate-induced currents.

Data analysis. Experiments with the mammalian cell expression system were repeated at least three times with independent transfections, and uptake measurements were made in duplicate in each experiment. Experiments with the oocyte expression system were also repeated at least three times with different sets of oocytes. The kinetic constants (K_t and V_{max}) were calculated independently each time the experiment was repeated. The kinetic parameters were calculated using the commercially available computer program Sigma Plot, version 6.0 (SPSS, Chicago, IL). We used the unpaired two-sample t test to determine whether the difference in kinetic parameters between any given pair of experimental conditions was statistically significant; a $p < 0.05$ was considered statistically significant. Data are given as means ± S. E.

Results

Cloning and functional characterization of chimpanzee, Rhesus monkey, dog, and zebrafish NaCTs. We cloned chimpanzee NaCT cDNA from liver RNA and the protein, predicted by the sequence of the coding region of the cDNA, consisted of 568 amino acids

(GenBank accession no. HM_998308), which was equal to the number of amino acids in human NaCT. Sequence comparison between human and chimpanzee NaCTs showed 99% identity. There were only three amino acid differences between the transporters from the two species. The Rhesus monkey (*Macaca mulatta*) NaCT cDNA was cloned from liver, and the sequence predicted a protein consisting of 568 amino acids (GenBank accession no. HM_998307), similar to human and chimpanzee NaCTs. Sequence comparison between human and Rhesus monkey NaCTs showed 97% identity. There were only sixteen amino acid differences between the transporters from the two species. The dog NaCT cDNA was cloned from liver, and the predicted amino acid sequence was 100% identical to the sequence already reported in the GenBank. Sequence comparison between human and dog NaCTs showed 84% identity and 91% similarity. We cloned zebrafish NaCT cDNA from a cDNA library prepared using poly(A) RNA isolated from whole zebrafish. The cDNA is 2,551-bp long with an open reading frame coding for 582 amino acids (GenBank accession no. HM_998309). Sequence comparison between human and zebrafish NaCTs showed 61% identity and 78% similarity.

We have previously characterized the transport function of rat, mouse, and human NaCTs (Inoue et al., 2002a,b; 2004). Here we examined the functional features of the newly cloned chimpanzee, monkey, dog, and zebrafish NaCTs using a mammalian cell expression system. NaCTs from all these four species mediated citrate uptake (Supplemental Figure 1). In each case, the cDNA-induced citrate uptake was obligatorily dependent on Na^+ (Supplemental Figure 2). Substrate selectivity was then examined by monitoring the abilities of unlabeled citrate, succinate, α-ketoglutarate, malate, and lactate to compete with [^{14}C]-citrate (10 μM) for the cDNA-induced uptake process (Supplemental Figure 3). At a concentration of 2.5 mM, citrate, succinate, and malate caused significant inhibition of [^{14}C]-citrate uptake induced by chimpanzee

JPET Fast Forward. Published on January 23, 2015 as DOI: 10.1124/jpet.114.221523
This article has not been copyedited and formatted. The final version may differ from this version.

and monkey NaCT cDNAs. Citrate was the most potent inhibitor. α-Ketoglutarate and lactate had little or no effect. Similar results were obtained with dog and zebrafish NaCT cDNAs except that the inhibition with citrate, succinate, and malate was much greater than that seen with chimpanzee and monkey NaCTs. In addition, α-ketoglutarate, which had little effect on citrate uptake mediated by chimpanzee and monkey NaCTs, was a potent inhibitor of citrate uptake mediated by dog and zebrafish NaCTs. We also found that unlabeled citrate inhibited [^{14}C]-citrate uptake mediated by dog and zebrafish NaCTs much more than [^{14}C]-citrate uptake mediated by chimpanzee and monkey NaCTs.

Differential influence of Li^+ on primate versus non-primate NaCTs. We studied the effects of Li^+ on the transport function of NaCTs from eight different species (primates: human, chimpanzee, and monkey; non-primates: mouse, rat, dog, zebrafish, and *C. elegans*). We have shown previously that Li^+ stimulates human NaCT, inhibits mouse, rat, and zebrafish NaCTs, and has no effect on *C. elegans* NaCT (Inoue et al., 2003). These studies were done with a single concentration of Li^+ (2 mM). In the present study, we examined the dose-response relationship for the influence of Li^+ on NaCTs from different species (Fig. 1). The activities of the primate NaCTs were stimulated by Li^+ (Fig. 1A). In contrast, the activities of non-primate NaCTs were inhibited by Li^+ (Fig. 1B). *C. elegans* NaCT was not affected by Li^+ over a concentration range of 1-20 mM. At a concentration of 2.5 mM, Li^+ increased the activities of chimpanzee and human NaCTs approximately 3-fold. Monkey NaCT was stimulated 2-fold under similar conditions. With non-primate NaCTs, 2.5 mM Li^+ caused 30-40% inhibition. We have previously shown that Li^+ stimulates human NaCT by converting the transporter from a low-affinity/high-capacity type to a high-affinity/low-capacity type (Inoue et al., 2003). A similar phenomenon occurs with the other two primate NaCTs (Fig. 2). For chimpanzee NaCT-mediated

JPET Fast Forward. Published on January 23, 2015 as DOI: 10.1124/jpet.114.221523
This article has not been copyedited and formatted. The final version may differ from this version.

citrate uptake, the K_t and V_{max} values were 820 ± 117 μM and 1162 ± 115 pmoles/10^6 cells/min in the absence of Li^+; the corresponding values in the presence of 10 mM Li^+ were 36 ± 8 μM and 291 ± 28 pmoles/10^6 cells/min (Fig. 2A). For monkey NaCT-mediated citrate uptake, the K_t and V_{max} values were 224 ± 14 μM and 640 ± 18 pmoles/10^6 cells/min in the absence of Li^+; the corresponding values in the presence of 10 mM Li^+ were 53 ± 10 μM and 199 ± 21 pmoles/10^6 cells/min (Fig. 2B).

We also studied the differential influence of Li^+ on human NaCT versus rat NaCT using the electrophysilogical technique in the *X. laevis* oocyte expression system. We found that perifusion of human NaCT- or rat NaCT-expressing oocytes with citrate in the presence of Na^+ induced marked inward currents and that such currents were not detectable when Na^+ in the perifusion buffer was replaced with Li^+. This shows that Li^+ does not substitute for Na^+ to support the activity of NaCT. However, in the presence of Na^+, Li^+ increased the magnitude of Na^+/citrate-induced currents for human NaCT but decreased the magnitude of Na^+/citrate-induced currents for rat NaCT (Fig. 3). Analysis of the dose-response relationship revealed that the stimulation for human NaCT was approximately 2.5-fold at 2.5 mM Li^+. The magnitude of stimulation increased further with increasing concentrations of Li^+; the stimulation observed at 20 mM Li^+ was approximately 6-fold. For rat NaCT, the inhibition was ~40% at 2.5 mM Li^+, and it increased further with increasing concentrations of Li^+ (~85% inhibition at 20 mM Li^+). We then analyzed the influence of Li^+ on the substrate affinity of human NaCT (Fig. 4). In the absence of Li^+, the citrate saturation kinetics for human NaCT conformed to the Michaelis-Menten equation describing a single saturable system; the Eadie-Hofstee plot was linear and the K_t for citrate was 6.6 ± 0.2 mM (Fig. 4A). In the presence of Li^+ (10 mM), the citrate-induced currents increased in magnitude, and the currents were saturable with increasing concentrations of citrate.

JPET Fast Forward. Published on January 23, 2015 as DOI: 10.1124/jpet.114.221523
This article has not been copyedited and formatted. The final version may differ from this version.

Interestingly, the saturation kinetics did not conform to the Michaelis-Menten equation describing a single saturable system. The Eadie-Hofstee plot was curvilinear, indicating the presence of more than one saturable system (Fig. 4B). Indeed, the data fit to the Michaelis-menten equation describing a combination of two saturable systems. The K_t values for citrate for the two systems were 8.1 ± 1.7 mM (low-affinity system) and 0.69 ± 0.04 mM (high-affinity system).

We then evaluated the influence of Li^+ on the kinetic parameters of rat NaCT using the oocyte expression system by following its transport activity electrophysiologically. The citrate-induced currents were decreased in the presence of Li^+, but the currents were saturable with increasing concentrations of citrate both in the absence and presence of Li^+ (Fig. 5). Interestingly, the influence of Li^+ on rat NaCT was not associated with any significant change in the affinity for citrate. The K_t value for citrate was 44 ± 7 μM in the absence of Li^+; the value did not change in the presence of 10 mM Li^+ (43 ± 4 μM).

Influence of H^+on the transport activity of human NaCT. Since Lithium (atomic number, 3) is closest to Hydrogen (atomic number, 1) in the Periodic Table and also because Li^+ substitutes for H^+ in certain transporters (e.g., Na^+/H^+ exchanger), we asked whether H^+ is capable of stimulating Na^+-coupled citrate uptake mediated by human NaCT. To address this question, we first analyzed the influence of pH on the transport function of human NaCT using the mammalian cell expression system (Fig. 6A). We found the extracellular pH to have a profound effect on NaCT activity. Increasing the concentration of H^+ in the uptake buffer enhanced the activity of human NaCT markedly. Changing the pH from 8.5 to 6.5 increased the activity 7-fold. The optimum pH for human NaCT was 6.5. Further acidification of the uptake buffer decreased the activity. Since extracellular pH is also expected to change the ionic state of

citrate, it is difficult to interpret the observed H^+-induced increase in transport activity. Therefore, we compared the magnitude of Li^+ (10 mM)-induced stimulation of human NaCT at three different H^+ concentrations: 3.16 nM (pH, 8.5), 31.6 nM (pH, 7.5), and 316 nM (pH, 6.5) (Fig. 6B). The stimulation was 4.7-fold at pH 8.5, 3.6-fold at pH 7.5, and 1.6-fold at pH 6.5.

Role of Phe-500 in human NaCT in Li^+-induced stimulation of transport activity. Phenylalanine at position 500 in human NaCT is critical for Li^+-induced stimulation of transport activity (Inoue et al., 2003). Substitution of leucine for phenylalanine at this position (F500L) stimulates the transport activity and also almost completely abolishes Li^+ stimulation (Inoue et al., 2003). Here we evaluated the influence of nine different amino acid substitutions for Phe-500 in human NaCT on the transport activity and also on Li^+-induced stimulation (Table I). Substitution with charged amino acids aspartate (F500D) or lysine (F500K) decreased the transport activity markedly, but the remaining residual activity was still stimulated by Li^+. Substitution with tyrosine (F500Y) also decreased the transport activity, and the ability of Li^+ to stimulate the remaining residual activity was still intact. Upon substitution with other neutral amino acids, the influence on basal activity varied between almost no effect (F500A) and a robust stimulation (8.3-fold stimulation for F500W). Interestingly, the greater the basal activity, the lesser was the Li^+-induced stimulation. While the wild type human NaCT was stimulated 6-fold by 10 mM Li^+, the activity of the F500W mutant was not at all affected. There was a reciprocal correlation between the basal activity and the magnitude of Li^+ stimulation for all amino acid substitutions ($r^2 = -0.92$).

Comparison of the effects of Li^+ between wild type and F500W mutant human NaCTs. The primary mechanism by which Li^+ stimulates human NaCT is by increasing the substrate affinity. Since the F500W mutant human NaCT has greatly increased basal activity and is not

stimulated by Li^+, we asked whether the substitution of phenylalanine at position 500 with tryptophan alters the transporter's affinity for citrate by converting the transporter from a low-affinity type to a high-affinity type. To address this question, we analyzed the kinetic parameters of citrate uptake by wild type and F500W mutant human NaCTs using the mammalian cell expression system in the absence and presence of Li^+ (10 mM). The K_t and V_{max} values for the wild type human NaCT were 586 ± 47 μM and 738 ± 38 pmoles/10^6 cells/min in the absence of Li^+ (Fig. 7A). The corresponding values in the presence of Li^+ were 62 ± 8 μM and 210 ± 15 pmoles/10^6 cells/min (Fig. 7B), indicating that Li^+-induced stimulation of wild type NaCT transport activity is associated with the conversion of the transporter from a low-affinity/high-capacity type to a high-affinity/low-capacity type. The K_t and V_{max} values for the F500W mutant human NaCT were 23 ± 3 μM and 170 ± 11 pmoles/10^6 cells/min in the absence of Li^+ (Fig. 7C). The corresponding values in the presence of Li^+ were 20 ± 5 μM and 56 ± 5 pmoles/10^6 cells/min (Fig. 7D). These data show that substitution of phenylalanine at position 500 with tryptophan converts the transporter from a low-affinity/high-capacity type to a high-affinity/low-capacity type even in the absence of Li^+. The presence of Li^+ elicits only a minor influence on the kinetic parameters of the mutant human NaCT, indicating that the F500W mutant human NaCT behaves in the absence of Li^+ kinetically similar to wild type human NaCT in the presence of Li^+.

Comparison of the effects of H^+ between wild type and F500W mutant human NaCTs. Since Li^+ and H^+ elicit similar influence on the transport function of human NaCT, we analyzed the impact of various amino acid substitutions at position 500 in human NaCT on the stimulatory effect of H^+. We compared the transport activities of wild type and various mutant human NaCTs at pH 8.5 and pH 6.5 (Fig. 8). As seen with Li^+-induced stimulation, the amino acid substitutions

that increased the basal transport activity significantly decreased the magnitude of H^+-induced stimulation. The activity of wild type human NaCT increased 3 to 4-fold when the extracellular pH was changed from 8.0 to 6.5. In contrast, the F500W mutant human NaCT, which had almost 10 times higher basal activity compared to wild type human NaCT, responded only minimally when the extracellular pH was changed from 8.0 to 6.5. The other amino acid substitutions (F500L, F500M, F500V, and F500I), which increased the basal transport activity at an intermediate level, also showed significantly attenuated response to H^+-induced stimulation. We then analyzed the kinetic parameters of citrate uptake by wild type and F500W mutant human NaCTs under identical conditions using the mammalian cell expression system at pH 8.5 and pH 6.5. The K_t and V_{max} values for the wild type human NaCT were 2132 ± 169 μM and 872 ± 56 pmoles/10^6 cells/min at pH 8.5 (Fig. 9A). The corresponding values at pH 6.5 were 256 ± 18 μM and 573 ± 28 pmoles/10^6 cells/min (Fig. 9B), indicating that H^+-induced stimulation of wild type NaCT transport activity is associated with the conversion of the transporter from a low-affinity/high-capacity type to a high-affinity/low-capacity type. The K_t and V_{max} values for the F500W mutant human NaCT were 57 ± 4 μM and 147 ± 6 pmoles/10^6 cells/min at pH 8.5 (Fig. 9C). The corresponding values at pH 6.5 were 18 ± 5 μM and 147 ± 13 pmoles/10^6 cells/min (Fig. 9D). It is thus evident that H^+ elicits only a minor influence on the kinetic parameters of the F500W mutant human NaCT because the substitution of phenylalanine at this position with tryptophan itself increases the basal activity of the transporter by increasing its substrate affinity.

Discussion

Citrate is a critical metabolite at the center of many important metabolic pathways. Apart from its mitochondrial role in the Krebs cycle (tricarboxylic acid cycle) and the cytoplasmic role

as the source of acetyl CoA for the synthesis of fatty acids and cholesterol, it is also an important regulator of glycolysis by its ability to inhibit phosphofructo-1-kinase. The commonly accepted view regarding citrate in the cytoplasm is that after synthesis inside the mitochondria, citrate exits the mitochondrial matrix via the mitochondrial citrate carrier (SLC25A1) if appropriate metabolic conditions exist in the cell. It is generally considered that the mitochondrial citrate is the only source of citrate in the cytoplasm. Even though the levels of citrate in blood are significant (~160 μM), it is generally not taken into account as a possible source of cytoplasmic citrate in tissues that utilize citrate for the synthesis of fatty acids and cholesterol. The discovery of NaCT as a plasma membrane transporter that is capable of uphill transfer of citrate from the circulation into the cytoplasm of the cells (Inoue et al., 2002a,b; 2004) indicates that the blood-borne citrate is also likely an important source of cytoplasmic citrate in mammalian cells. Liver is the major organ where the activities of the cytoplasmic metabolic pathways involving citrate are robust, and this is the tissue where NaCT is expressed most abundantly (Inoue et al., 2002a,b; 2004). The sinusoidal location of the transporter in the hepatocytes (Gopal et al., 2007) is appropriate for this postulated role. The potential role of NaCT in channeling circulating citrate into important biochemical pathways in the liver may have biological consequences. NaCT was discovered in mammals as the result of the discovery of a citrate transporter in *Drosophila*, which has a critical role as an important determinant of lifespan in this organism (Rogina et al., 2000). The *Drosophila* transporter, known as Indy, is expressed most abundantly in fat body, the organ equivalent to the liver in mammals (Rogina et al., 2000). Even though the role of *Indy* as a lifespan-determining gene has been questioned (Toivonen et al., 2007), many studies have shown convincingly that the transporter does indeed play a role as a modulator of lifespan not only in *Drosophila* (Marden et al., 2003; Neretti et al., 2009; Wang et al., 2009) but also in *C. elegans*

(Fei et al., 2004). Even though the relevance of NaCT to lifespan in mammals remains yet to be determined, it is likely that this transporter plays an essential role in important metabolic pathways. This is supported by metabolic studies in *Slc13a5*-null mice, which show that the absence the transporter protects against diet-induced adiposity, insulin resistance, and metabolic syndrome (Birkenfeld et al., 2011).

In the present study, we cloned NaCT from four additional species (chimpanzee, monkey, dog, and zebrafish) and characterized their function. There is a single entry in the GenBank (accession no. XM_511987) predicting the amino acid sequence of chimpanzee (*Pan troglodytes*) NaCT. The predicted protein consists of 475 amino acids, 93 amino acids shorter than human NaCT cloned in our laboratory (GenBank accession no. XM_137672). This indicates that the chimpanzee NaCT in the GenBank database (XM_511987) represents a truncated protein. This was confirmed by the sequence of the chimpanzee NaCT cloned in the present study. There are four entries in the GenBank (accession no. XM_2763975, XM_2763976, XM_2763977, and XM_2763978) predicting the amino acid sequence of marmoset (*Callithrix jacchus*) NaCT, each prediction giving a different number of amino acids (571, 554, 528 or 525) in the protein. There was no information on monkey NaCT. The present study is the first to report on the sequence of monkey NaCT. The sequence of dog NaCT already exists in GenBank, and the dog NaCT cDNA cloned in the present study is identical to the one present in the GenBank.

We analyzed the transport function of the newly cloned chimpenzee, monkey, dog, and zebrafish NaCTs and compared the functional features among the four species. Even though NaCTs from all four species were absolutely Na^+-dependent, chimpanzee and monkey NaCTs were relatively more selective for citrate than dog and zebrafish NaCTs, and chimpanzee and

monkey NaCTs showed lower affinity for citrate than dog and zebrafish NaCTs. Li^+ stimulated the activity of only chimpanzee and monkey NaCTs as was the case with human NaCT; in contrast, Li^+ inhibited the activity of dog and zebrafish NaCTs.

With human NaCT expressed in *Xenopus laevis* oocytes, two kinetically distinguishable transport components were evident in the presence of Li^+. The low-affinity system apparently corresponded to the system in the absence of Li^+ whereas the high-affinity system apparently represented the Li^+-stimulated system. The presence of Li^+ did convert human NaCT from a relatively low-affinity system to a high-affinity system, but the conversion was not homogeneous. The high-affinity population had bound Li^+ with consequent change in citrate affinity whereas the low-affinity population apparently did not have bound Li^+ and hence showed no change in citrate affinity. These findings are in contrast to the results from the mammalian cell expression system where the conversion of human NaCT in the presence of Li^+ from a low-affinity system to a high-affinity system was complete. Another notable difference between the oocyte expression system and the mammalian cell expression system was in the Michaelis constant for citrate. In the absence of Li^+, the K_t for citrate was 0.60 ± 0.07 mM in the mammalian cell expression system; the value was almost 10 times higher (6.6 ± 0.2 mM) in the oocyte expression system.

The transport function of rat NaCT was inhibited by Li^+. The inhibition was associated solely with a decrease in the maximal velocity of the transport system. This contrasted the influence of Li^+ on human NaCT where the influence of Li^+ was on the affinity for citrate by converting the transporter from a low-affinity/high-capacity type to a high-affinity/low-capacity type. Another notable difference between human NaCT and rat NaCT when analyzed using the mammalian cell expression system and the oocyte expression system was in the effect of the expression system

on substrate affinity. With human NaCT, the affinity for citrate was 10 times poorer in the oocyte expression system than in the mammalian cell expression system. With rat NaCT however, the decrease in citrate affinity was only 2-fold.

In the present study, we also compared the effects of Li^+ and H^+ on the activity of human NaCT. In the presence of Na^+, increasing the concentrations of H^+ increased the activity of the transporter as was seen with Li^+. There was a competition between Li^+ and H^+ to elicit the stimulatory effect. The ability of Li^+ to stimulate the transport activity of human NaCT decreased with increasing $[H^+]$ because the transporter was activated by H^+ itself. This difference in Li^+-induced stimulation was independent of the pH-induced changes in the relative amounts of differently charged ionic species of citrate. This suggests that H^+ is able to substitute for Li^+ for the stimulation of human NaCT.

The salient feature of the present study is the discovery that the stimulatory effect of Li^+ is unique only to primate NaCTs. Li^+ inhibits non-primate NaCTs. The stimulatory effect of Li^+ on human NaCT is potent; the stimulation is more than 2-fold at a Li^+ concentration of 1 mM. These findings have clinical and therapeutic implications. Lithium is used widely in the treatment of affective disorders such as bipolar disorder. The plasma concentrations of Li^+ in patients receiving lithium treatment are in the range of 0.8 -2 mM (Sproule, 2002). Therefore, the activity of NaCT in patients treated with lithium is likely to be increased many-fold, enhancing the utilization of circulating citrate for the synthesis of fatty acids and cholesterol in the liver. Considering the fact that lithium is prescribed also in the form of lithium citrate, patients who take lithium in this form will not only have Li^+ in the circulation to activate NaCT in the liver but also have increased levels of citrate in the circulation as the substrate for NaCT. The findings that Li^+ activates the human transporter by increasing the affinity for citrate are also

JPET Fast Forward. Published on January 23, 2015 as DOI: 10.1124/jpet.114.221523
This article has not been copyedited and formatted. The final version may differ from this version.

physiologically relevant. Citrate is present in the circulation only at sub-saturating concentrations (K_t for citrate in the mammalian cell expression system, ~600 μM; K_t for citrate in the oocyte expression system, ~6 mM; plasma concentration of citrate, ~160 μM). Therefore, the Li^+-induced increase in the affinity will certainly enhance the entry of circulating citrate into liver cells under physiological conditions. The difference in substrate affinity for human NaCT between the mammalian cell expression system and the oocyte expression system is interesting. We have shown previously a similar difference between HepG2 cells and the mammalian cell expression system (Inoue et al., 2002b; Gopal et al., 2007). The human NaCT cDNA was isolated from a HepG2 cell cDNA library (Inoue et al., 2002b). When this cDNA was expressed in HRPE cells, the affinity for citrate was ~650 μM (Inoue et al., 2002b). But, when the activity of the constitutively expressed NaCT was monitored in HepG2 cells, the affinity for citrate was ~5 mM (Gopal et al., 2007). When the same transporter was expressed in oocytes in the present study, the affinity for citrate was ~6 mM. The reasons for this difference are not known, but we speculate that post-translational modifications of the transporter may have a role. The heterologous expression in HRPE cells is transient and the activity of the transporter is measured within 12 h of transfection with the transporter cDNA, a time frame that may not be conducive for effective post-translational modifications. In contrast, NaCT is expressed constitutively in HepG2 cells; even though we have no information on the half-life of the transporter protein in these cells, it is possible that the transporter resides in these cells long enough for post-translational modifications. In the oocyte expression system, the transporter activity is monitored 4-6 days after injection of the transporter cRNA, which may allow sufficient time for post-translational modifications. This may be the reason why the affinity for citrate is similar for the

human NaCT in the oocyte expression system and in HepG2 cells. The validity of this explanation remains to be determined in future studies.

The activation of human NaCT with therapeutically relevant concentrations of Li^+ has significant clinical implications. One of the unwanted side effects of lithium therapy in humans is the weight gain associated with an increase in the circulating levels of triglycerides and cholesterol (Bergmann et al., 2007; Bardini et al., 2009). Since NaCT facilitates the utilization of circulating citrate in liver cells for fatty acid and cholesterol synthesis, it is plausible that the Li^+-induced activation of this transporter underlies this side effect. Unfortunately, this cannot be tested in animal studies using mice or rats because rodent NaCTs are inhibited, not activated, by Li^+. The present findings that the Li^+-induced activation is specific for primate NaCTs preclude the use of mice or rats as suitable animal models to examine this mechanism. Non-human primates can be used for this purpose. Alternatively, transgenic mice expressing human NaCT in the liver instead of mouse NaCT (i.e., "humanized" mice) need to be generated to determine if activation of NaCT is the reason for the elevated levels of circulating triglycerides and cholesterol associated with lithium therapy.

The findings that substitution of phenylalanine at position 500 in human NaCT with other amino acids has profound influence on the transporter activity also have biological significance. The effects with these substitutions on the functional activity of NaCT are profound. Substitutions of Phe-500 with selective neutral amino acids increase the transporter activity whereas substitutions with charged amino acids decrease the activity. It is conceivable that polymorphisms at this particular position may have profound effects in humans with regard to NaCT activity and consequently may significantly influence the lipid profile.

Authorship Contributions

Participated in research design: E. Gopal, E. Babu, P. D. Prasad and V. Ganapathy

Conducted experiments: E. Gopal, E. Babu, S. Ramachandran and P. D. Prasad

Performed data analysis: E. Gopal, E. Babu, S. Ramachandran, Y.D Bhutia, P. D. Prasad and V. Ganapathy

Wrote or contributed to the writing of the manuscript: V. Ganapathy

References

Bardini G, Rotella CM, Giannini S, Harsch IA and Weimann A (2009) A link between hyperlipidemia and lithium? Confirmation of a recent previous observation. *Metabolism* 58: 735-737.

Bergmann T, Hahn EG, Harsch IA and Weimann A (2007) Lithium – a role in hyperlipidemia? *Metabolism* 56: 583-585.

Birkenfeld AL, Lee HY, Guebre-Egziabher F, Alves TC, Jurczak MJ, Jornayvaz FR, et al. (2011) Deletion of the mammalian INDY homolog mimics aspects of dietary restriction and protects against adiposity and insulin resistance in mice. *Cell Metab* 14: 184-195.

Fei YJ, Liu JC, Inoue K, Zhuang L, Miyake K, Miyauchi S and Ganapathy V (2004) Relevance of NAC-2, an Na^+-coupled citrate transporter, to life span, body size and fat content in *Caenorhabditis elegans*. *Biochem J* 379: 191-198.

Ganapathy V and Fei JY (2005) Biological role and therapeutic potential of NaCT, a sodium-coupled transporter for citrate in mammals. *Proc Ind Natl Sci Acad* B71: 83-96.

Gopal E, Miyauchi S, Martin PM, Ananth S, Srinivas SR, Smith SB, Prasad PD and Ganapathy V (2007) Expression and functional features of NaCT, a sodium-coupled citrate transporter, in human and rat livers and cell lines. *Am J Physiol Gastrointest Liver Physiol* 292: G402-G408.

Inoue K, Zhuang L, Maddox DM, Smith SB and Ganapathy V (2002a) Structure, function, and expression pattern of a novel sodium-coupled citrate transporter (NaCT) cloned from mammalian brain. *J Biol Chem* 277: 39469-39476.

Inoue K, Zhuang L and Ganapathy V (2002b) Human Na^+-coupled citrate transporter: primary structure, genomic organization, and transport function. *Biochem Biophys Res Commun* 299: 465-471.

Inoue K, Fei YJ, Huang W, Zhuang L, Chen Z and Ganapathy V (2002c) Functional identity of *Drosophila melanogaster* Indy as a cation-independent, electroneutral transporter for tricarboxylic acid-cycle intermediates. *Biochem J* 367: 313-319.

Inoue K, Zhuang L, Maddox DM, Smith SB, and Ganapathy V (2003) Human sodium-coupled citrate transporter, the orthologue of *Drosophila* Indy, as a novel target for lithium action. *Biochem J* 374: 21-26.

Inoue K, Fei JY, Gopal E, Miyauchi S, and Ganapathy V (2004) Functional features and genomic organization of mouse NaCT, a sodium-coupled transporter for tricarboxylic acid-cycle intermediates. *Biochem J* 378: 949-957.

Kline EE, Treat EG, Averna TA, Davis MS, Smith AY and Sillerud LO (2006) Citrate concentrations in human seminal fluid and expressed prostatic fluid determined via 1H nuclear magnetic resonance spectroscopy outperform prostate specific antigen in prostate cancer detection. *J Urol* 176: 2274-2279.

Knauf F, Rogina B, Jiang Z, Aronson PS and Helfand SL (2002) Functional characterization and immunolocalization of the transporter encoded by the life-extending gene Indy. *Proc Natl Acad Sci USA* 99: 14315-14319.

Knauf F, Mohebbi N, Teichert C, Herold D, Rogina B, Helfand SL, Gollasch M, Luft FC and Aronson PS (2006) The life-extending gene Indy encodes an exchanger for Krebs-cycle intermediates. *Biochem J* 397:25-29.

Kozlowski DJ, Chen Z, Zhuang L, Fei YJ, Navarre S and Ganapathy V (2008) Molecular characterization and expression pattern of taurine transporter in zebrafish during embryogenesis. *Life Sci* 82:1004-1011.

Marden JH, Rogina B, Montooth KL and Helfand SL (2003) Conditional tradeoffs between aging and organismal performanceof Indy long-lived mutant flies. *Proc Natl Acad Sci USA* 100: 3369-3373.

Markovich D and Murer H (2004) The SLC13 gene family of sodium sulphate/carboxylate cotransporters. *Pflugers Arch Eur J Physiol* 447: 594-602.

Neretti N, Wang PY, Brodsky AS, Nyguyen HH, White KP, Rogina B and Helfand SL (2009) Long-lived Indy induces reduced mitochondrial reactive oxygen species production and oxidative damage. *Proc Natl Acad Sci USA* 106: 2277-2282.

Pajor A (2006) Molecular properties of the SLC13 family of dicarboxylate and sulfate transporters. *Pflugers Arch Eur J Physiol* 451: 597-605.

Rogina B, Reenan RA, Nilsen SP and Helfand SL (2000) Extended life span conferred by cotransporter gene mutations in *Drosophila*. *Science* 290: 2137-2140.

Sproule B (2002) Lithium in bipolar disorder: can drug concentrations predict therapeutic effect? *Clin Pharmacokinet* 41: 639-660

Toivonen JM, Walker GA, Martinez-Diaz P, Bjedov I, Driege Y, Jacobs HT, Gems D and Partridge L (2009) No influence of Indy on lifespan in Drosophila after correcting for genetic and cytoplasmic background effects. *PLoS Genet* 3, e95.

Wada M, Shimada A and Fujita T (2006) Functional characterization of Na^+-coupled citrate transporter NaC2/NaCT expressed in primary cultures of neurons from mouse cerebral cortex. *Brain Res* 1081: 92-100.

Wang PY, Neretti N, Whitaker R, Hosier S, Chang C, Lu D, Rogina B and Halfand SL (2009) Long-lived Indy and calorie restriction interact to extend life span. *Proc Natl Acad Sci USA* 106: 9262-9267.

Wu X, Huang W, Prasad PD, Seth P, Rajan DP, Leibach FH, Chen J, Conway SJ and Ganapathy V (1999) Functional characteristics and tissue distribution pattern of organic cation transporter 2 (OCTN2), an organic cation/carnitine transporter. *J Pharmacol Exp Ther* 290: 1482-1492.

Yodoya E, Wada M, Shimada A, Katsukawa H, Okada N, Yamamoto A, Ganapathy V and Fujita T (2006) Functional and molecular identification of sodium-coupled dicarboxylate transporters in rat primary cultured cerebrocortical astrocytes and neurons. *J Neurochem* 97: 162-173.

Figure Legends

Figure 1. Differential influence of Li^+ on the activity of NaCTs from eight different species. NaCT cDNAs from different species were expressed heterologously in HRPE cells. The activity of the expressed transporters was monitored by measuring the uptake of [^{14}C]-citrate (10 μM) in a NaCl-containing buffer in the presence of varying concentrations of Li^+ (LiCl). Osmolality was maintained by adding appropriate concentrations of NMDG chloride. Data (means ± S. E.) represent cDNA-specific uptake. For each species, the results are expressed as percent of the corresponding cDNA-specific uptake measured in the absence of Li^+.

Figure 2. Influence of Li^+ on the kinetic parameters of chimpanzee and monkey NaCTs. Chimpanzee and monkey NaCT cDNAs were expressed in HRPE cells. The activity of the expressed transporters was monitored by the uptake of citrate over a concentration range of 10 - 2500 μM in a NaCl-containing buffer in the absence and presence of 10 mM Li^+ (LiCl). Osmolality was maintained by adding 10 mM NMDG chloride to the control buffer. Data (means ± S. E.) represent cDNA-specific uptake and are given in the form of Eadie-Hofstee plots (uptake rate/citrate concentration versus uptake rate). V, uptake rate; S, citrate concentration in mM.

Figure 3. Differential influence of Li^+ on human and rat NaCTs. Human and rat NaCTs were expressed heterologously in the *X. laevis* oocyte expression system. The activity of the expressed transporters was monitored using the two-microelectrode/voltage-clamp technique in a NaCl-containing buffer. Li^+ concentration was varied over a range of 0 – 20 mM in the form of LiCl.

Osmolality of the perifusion buffer was maintained by adding appropriate concentrations of NMDG chloride. The experiment was repeated with four different oocytes. The citrate-induced current measured in the absence of Li^+ was taken as 100%; the currents in the presence of Li^+ are given as percent of these control values. There were no measurable citrate-induced currents in uninjected oocytes. Data represent means ± S. E.

Figure 4. Influence of Li^+ on the kinetic parameters of human NaCT. Human NaCT was expressed in *X. laevis* oocytes. The activity of the expressed transporter was monitored using the two-microelectrode/voltage-clamp technique in a NaCl-containing buffer in the absence (A) and presence (B) of Li^+ (10 mM) in the form of LiCl. Osmolality of the perifusion buffer was maintained in control experiments by adding 10 mM NMDG chloride. The citrate-induced currents were measured over a concentration range of 0.25 – 15 mM. The experiment was repeated with four different oocytes. To normalize the variations in the levels of the heterologously expressed transporter in different oocytes, the current induced by 15 mM citrate in each oocyte was taken as 1, and the currents induced at other concentrations of citrate in a given oocyte were expressed as fractions of this value. *Inset*: Eadie-Hofstee plot. Data represent means ± S. E.

Figure 5. Influence of Li^+ on the kinetic parameters of rat NaCT. Rat NaCT was expressed in *X. laevis* oocytes. The activity of the expressed transporter was monitored using the two-microelectrode/voltage-clamp technique in a NaCl-containing buffer in the absence and presence of Li^+ (10 mM) in the form of LiCl. Osmolality of the perifusion buffer was maintained in control experiments by adding 10 mM NMDG chloride. The citrate-induced currents were

measured over a concentration range of 5 – 500 μM. The experiment was repeated with three different oocytes. Data represent means ± S. E.

Figure 6. Influence of extracellular pH on the activity of human NaCT and on the ability of Li^+ to stimulate the transporter. Human NaCT cDNA was expressed in HRPE cells. The activity of the expressed transporter was monitored by the uptake of citrate (10 μM) in a NaCl-containing buffer. (A) Uptake was measured at different pH, which was varied between 5.5 and 8.5 by adjusting the concentrations of Tris, Hepes, and Mes. (B) Uptake was measured at three different pH values (6.5, 7.5, and 8.5) in the absence and presence of Li^+ (10 mM). Osmolality of the uptake buffer was maintained by adding 10 mM NMDG chloride to the control buffer. Data (means ± S. E.) represent cDNA-specific uptake.

Figure 7. Comparison of Li^+ effects on kinetic parameters between wild type (F500) and F500W mutant human NaCTs. Wild type and mutant NaCT cDNAs were expressed in HRPE cells. The activity of the expressed transporters was monitored by the uptake of citrate over a given concentration range in a NaCl-containing buffer in the absence and presence of 10 mM Li^+ (LiCl). Osmolality was maintained by adding 10 mM NMDG chloride to the control buffer. The range of citrate concentrations varied depending on the transporter: 100 – 2500 μM for wild type human NaCT in the absence of Li^+ (A); 10 – 500 μM for wild type human NaCT in the presence of Li^+ (B); 5 – 250 μM for F500W mutant human NaCT in the absence of Li^+ (C); 10 – 500 μM for F500W mutant human NaCT in the presence of Li^+ (D). Data (means ± S. E.) represent cDNA-specific uptake.

Figure 8. Influence of extracellular pH on the activity of wild type and mutant human NaCTs. Wild type and mutant NaCT cDNAs were expressed in HRPE cells. The activity of the expressed transporter was monitored by the uptake of citrate (10 μM) in a NaCl-containing buffer at two different pH values: 6.5 and 8.0. Data (means ± S. E.) represent cDNA-specific uptake.

Figure 9. Comparison of the effects of extracellular pH on kinetic parameters between wild type (F500) and F500W mutant human NaCTs. Wild type and mutant NaCT cDNAs were expressed in HRPE cells. The activity of the expressed transporters was monitored by the uptake of citrate over a given concentration range in a NaCl-containing buffer at two different pH values: 6.5 and 8.5. The range of citrate concentrations varied depending on the transporter: 50 – 2500 μM for wild type human NaCT at pH 8.5 (A); 10 – 500 μM for wild type human NaCT at pH 6.5 (B); 5 – 250 μM for F500W mutant human NaCT at pH 8.5 (C); 10 – 500 μM for F500W mutant human NaCT at pH 6.5 (D). Data (means ± S. E.) represent cDNA-specific uptake.

JPET Fast Forward. Published on January 23, 2015 as DOI: 10.1124/jpet.114.221523
This article has not been copyedited and formatted. The final version may differ from this version.

Table 1. Influence of Li^+ on the activity of the wild type and mutant human NaCTs

Wild type and mutant human NaCT cDNAs were expressed in HRPE cells using the vaccinia virus expression technique, and the activity of the expressed transporters was monitored by the uptake of citrate (10 μM) in a NaCl-containing buffer in the absence and presence of Li^+ (10 mM). The experiments were repeated three times with independent transfections, and uptake measurements were made in duplicate in each experiment. Uptake of citrate in cells transfected with vector alone was negligible. Data (means ± S. E.) represent cDNA-specific uptake.

Amino acid substitution	Citrate uptake (pmoles/10^6 cells/min)		-Fold stimulation
	- Li^+	+ Li^+	
Wild type	0.31 ± 0.03	1.85 ± 0.19	6.0
F500L	1.67 ± 0.22	3.18 ± 0.45	1.9
F500A	0.32 ± 0.02	1.71 ± 0.11	5.4
F500D	0.05 ± 0.01	0.24 ± 0.05	5.3
F500K	0.06 ± 0.01	0.51 ± 0.11	8.6
F500M	1.12 ± 0.2	2.46 ± 0.33	2.2
F500V	0.42 ± 0.1	2.16 ± 0.46	5.2
F500W	2.58 ± 0.39	2.38 ± 0.19	0.9
F500Y	0.17 ± 0.01	1.07 ± 0.11	6.3
F500I	1.41 ± 0.09	2.71 ± 0.33	1.9

JPET Fast Forward. Published on January 23, 2015 as DOI: 10.1124/jpet.114.221523
This article has not been copyedited and formatted. The final version may differ from this version.

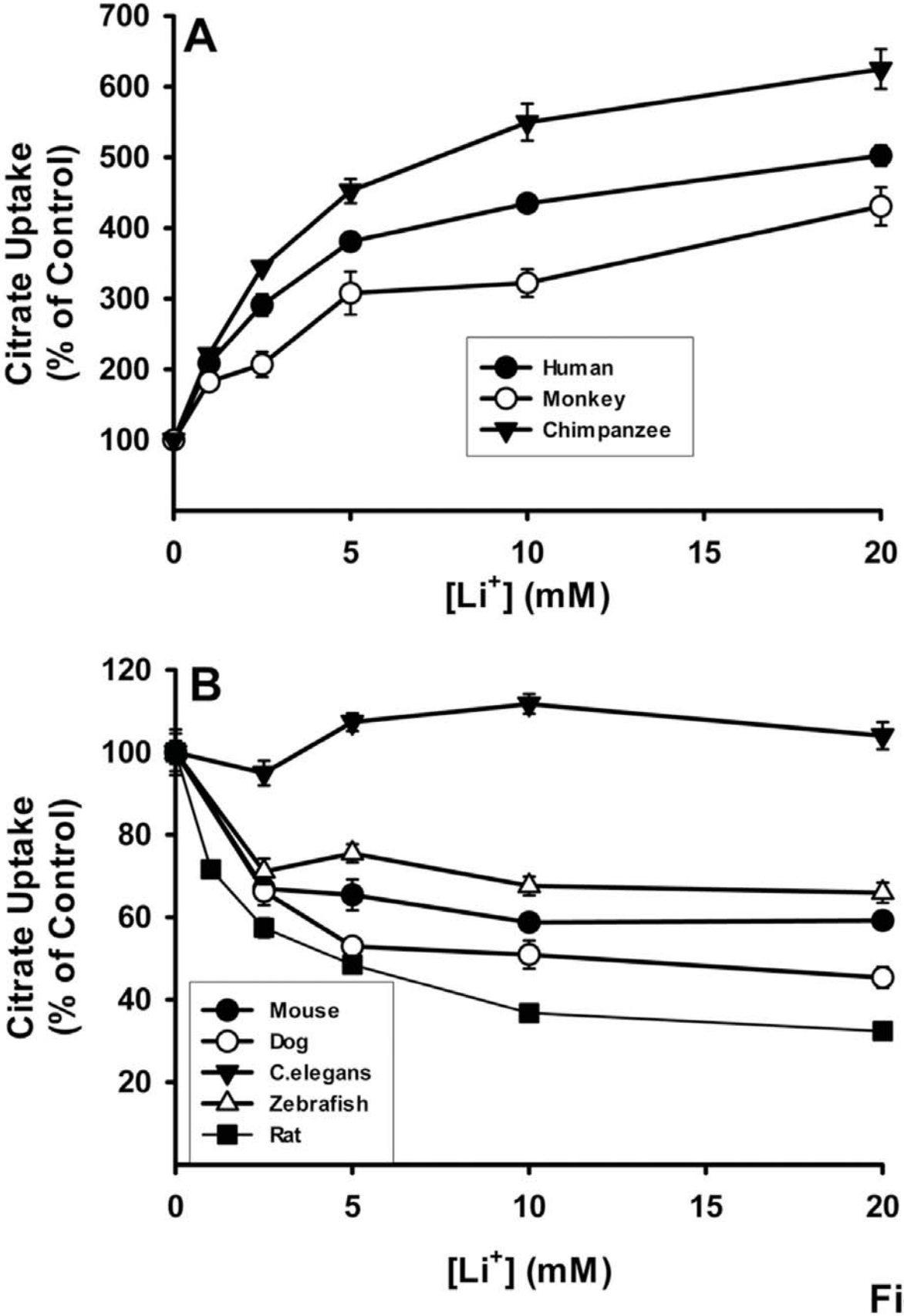

Fig. 1

JPET Fast Forward. Published on January 23, 2015 as DOI: 10.1124/jpet.114.221523
This article has not been copyedited and formatted. The final version may differ from this version.

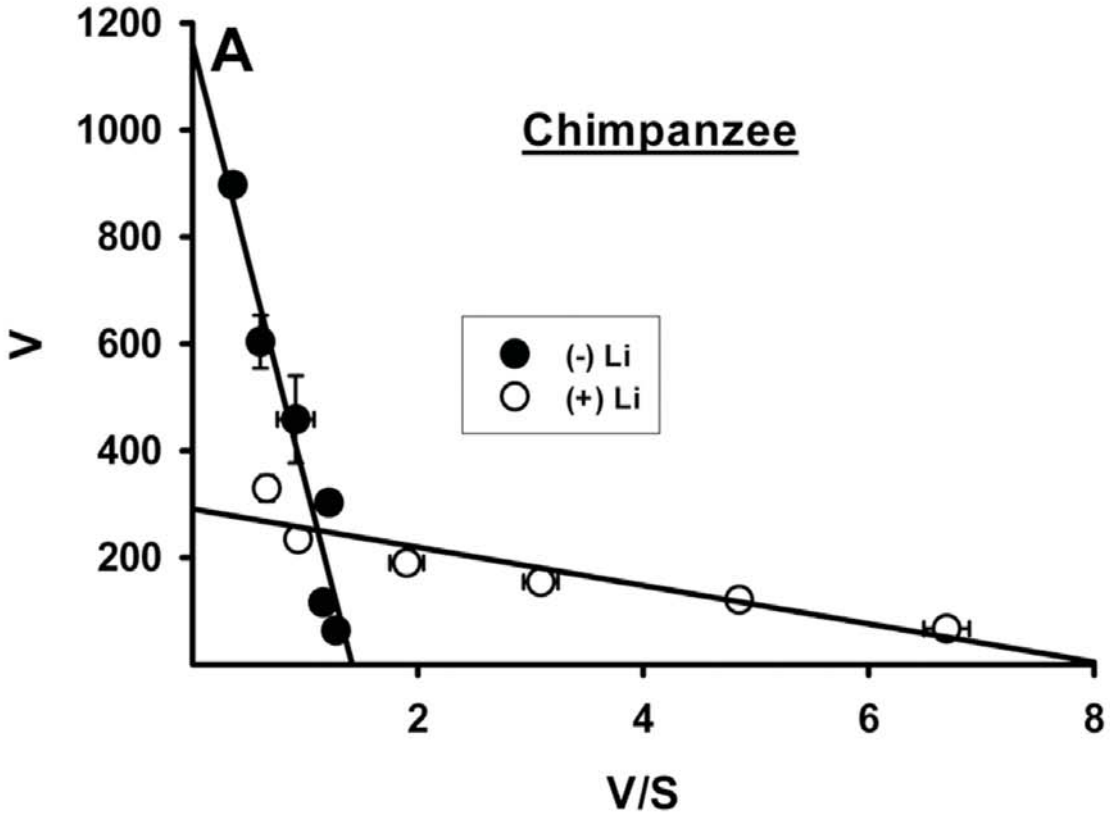

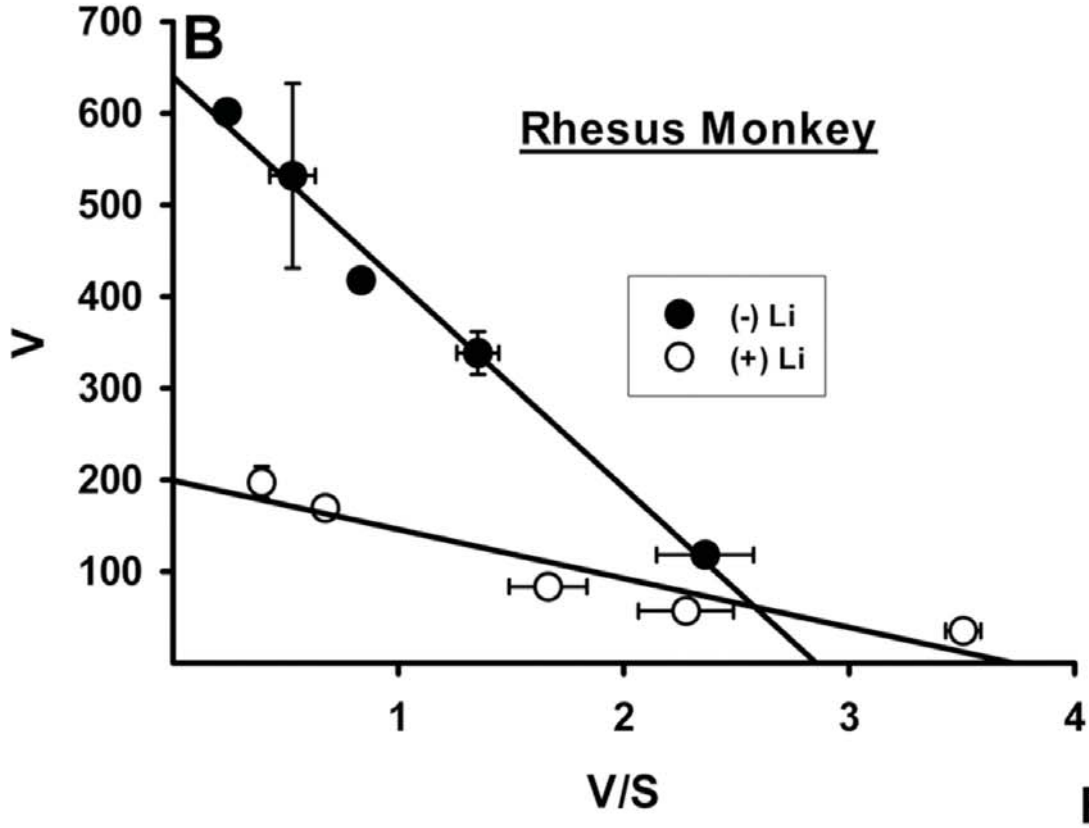

Fig. 2

JPET Fast Forward. Published on January 23, 2015 as DOI: 10.1124/jpet.114.221523
This article has not been copyedited and formatted. The final version may differ from this version.

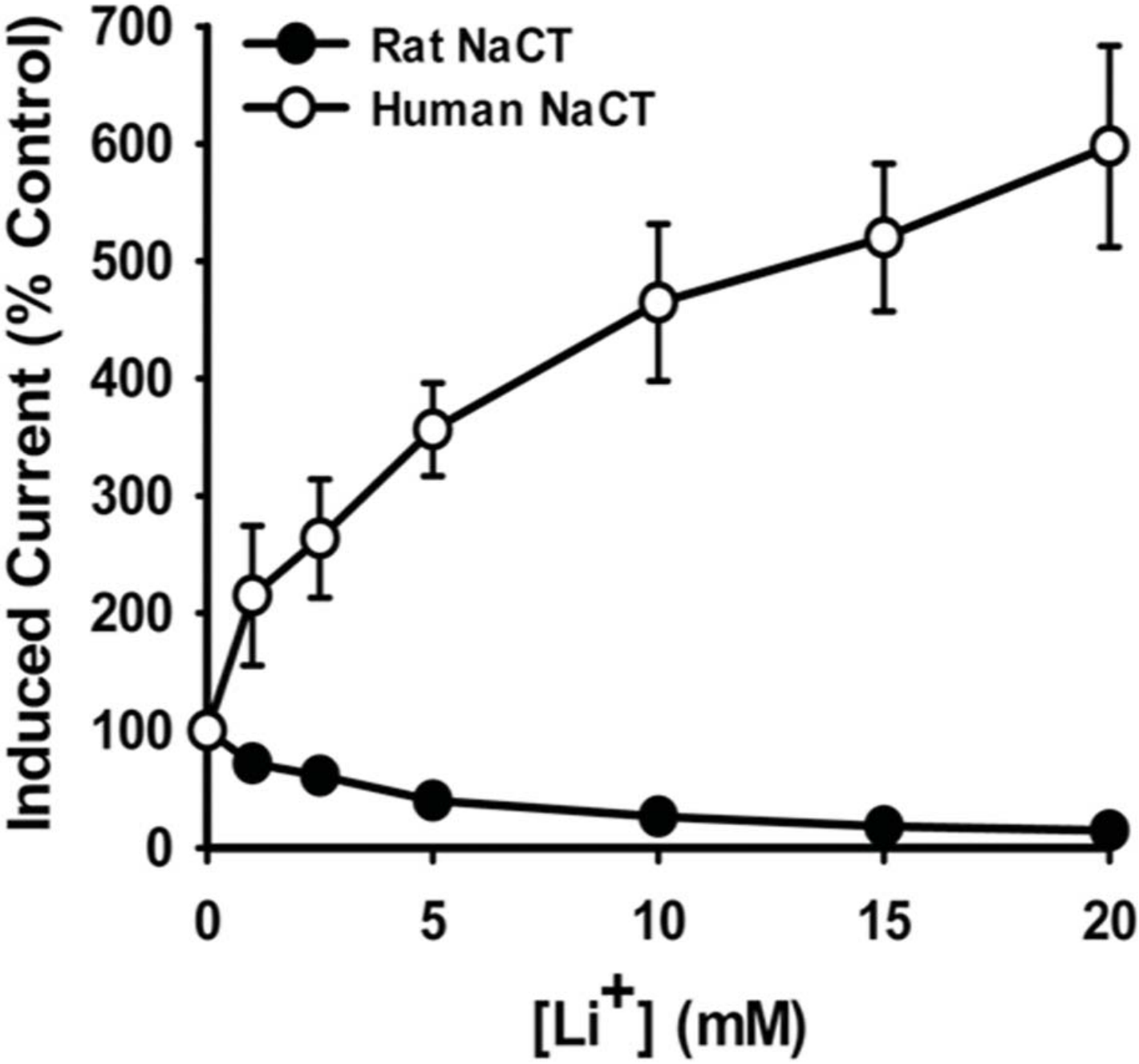

Fig. 3

JPET Fast Forward. Published on January 23, 2015 as DOI: 10.1124/jpet.114.221523
This article has not been copyedited and formatted. The final version may differ from this version.

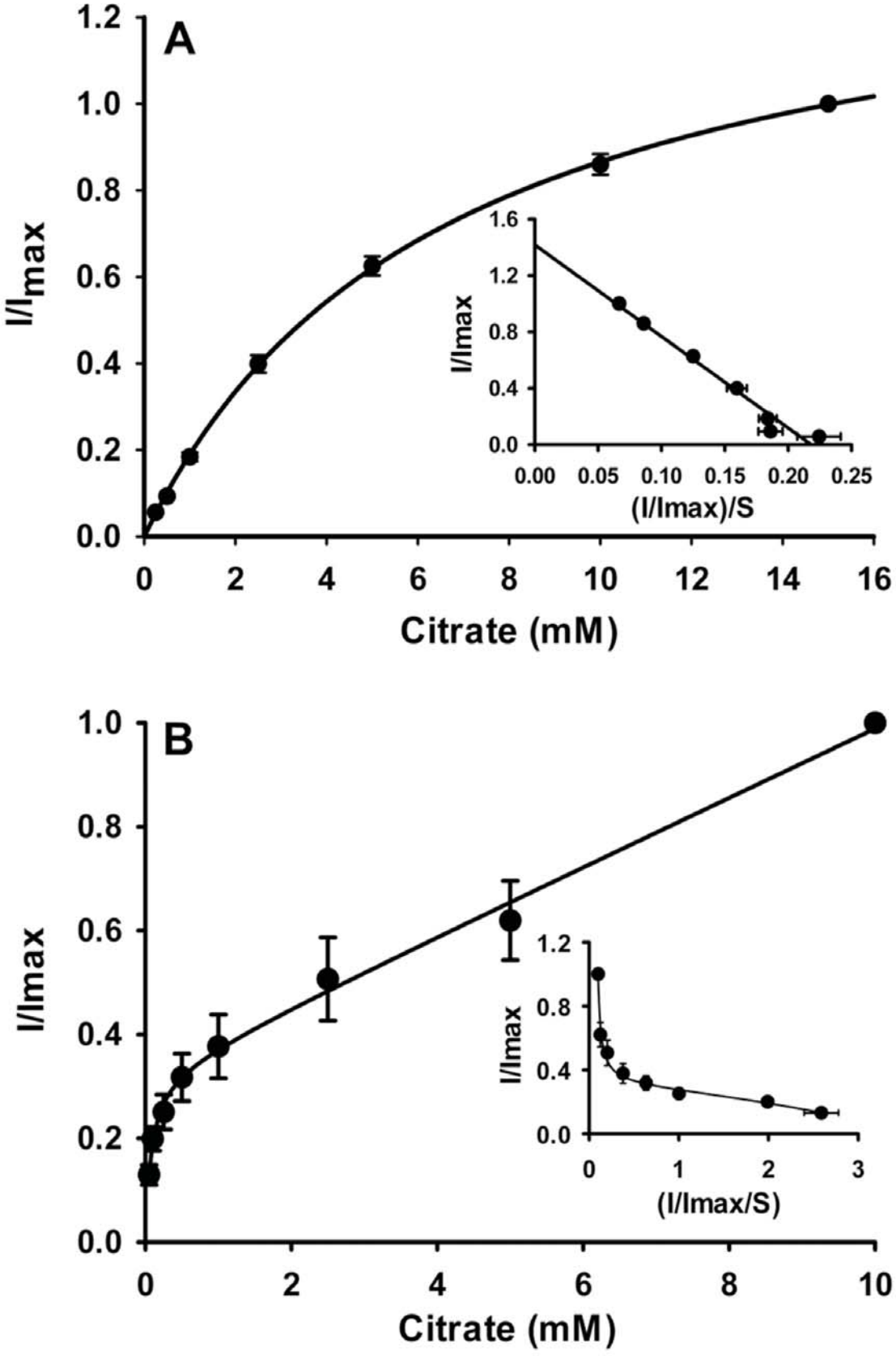

Fig. 4

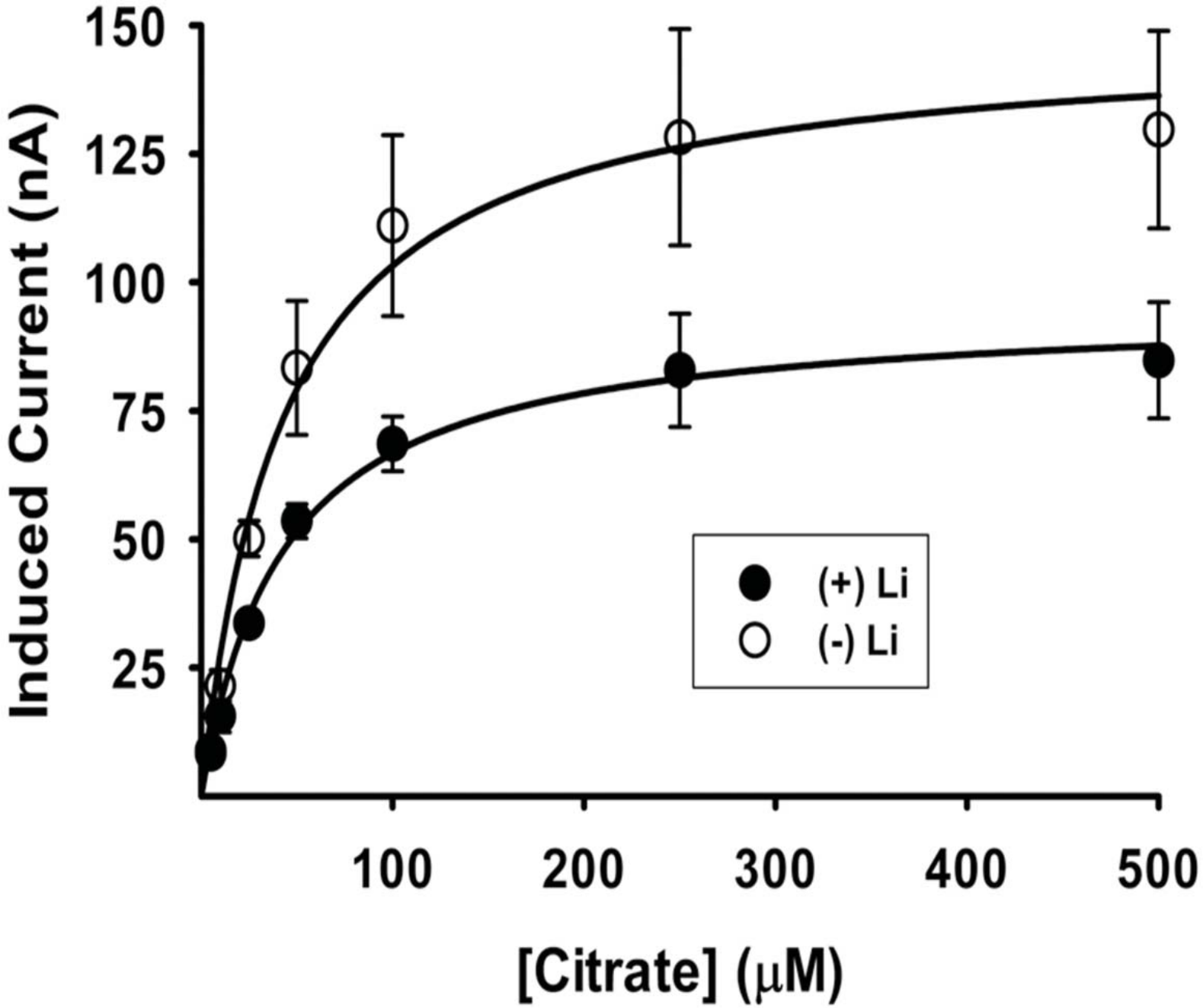

Fig. 5

JPET Fast Forward. Published on January 23, 2015 as DOI: 10.1124/jpet.114.221523
This article has not been copyedited and formatted. The final version may differ from this version.

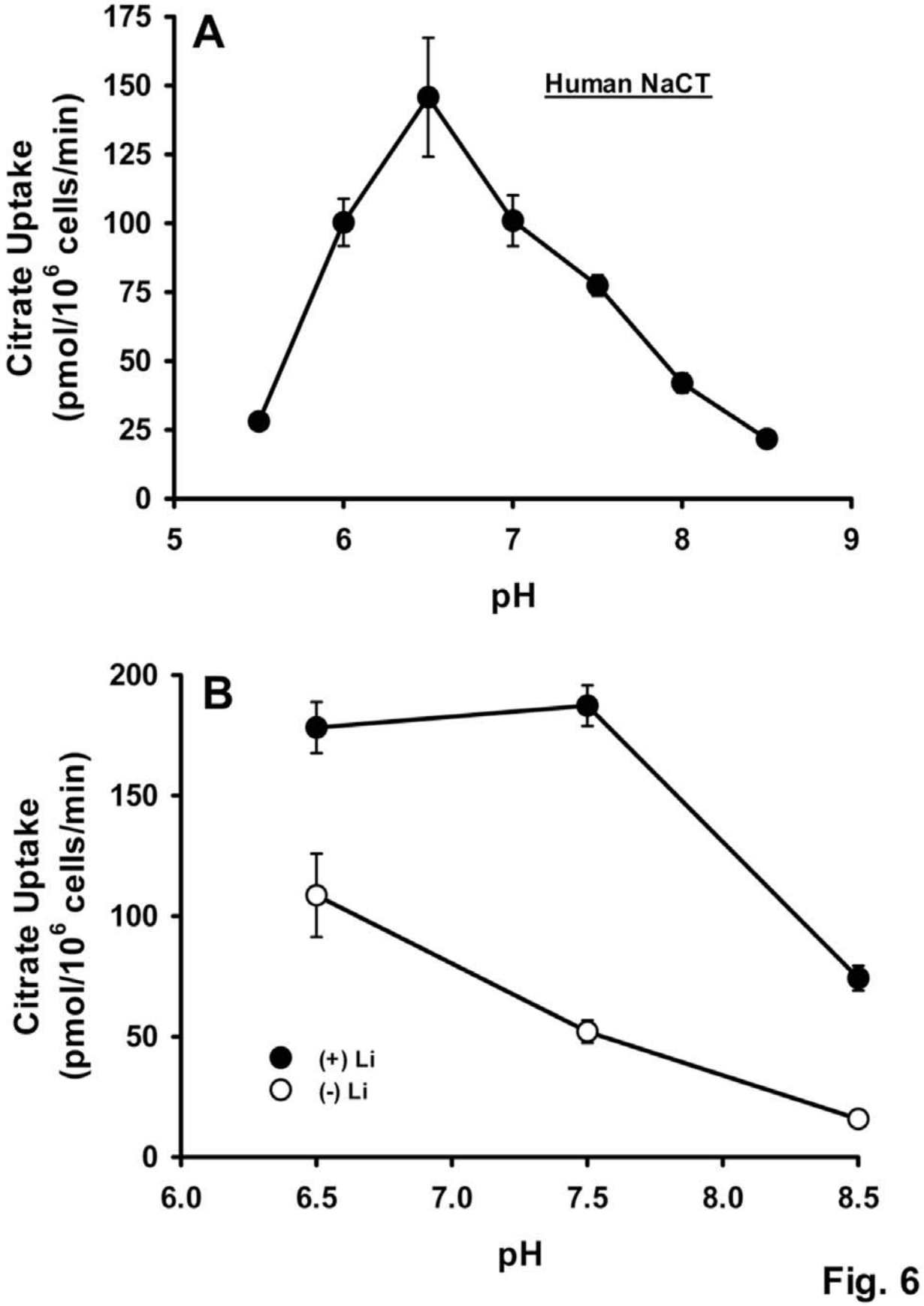

Fig. 6

JPET Fast Forward. Published on January 23, 2015 as DOI: 10.1124/jpet.114.221523
This article has not been copyedited and formatted. The final version may differ from this version.

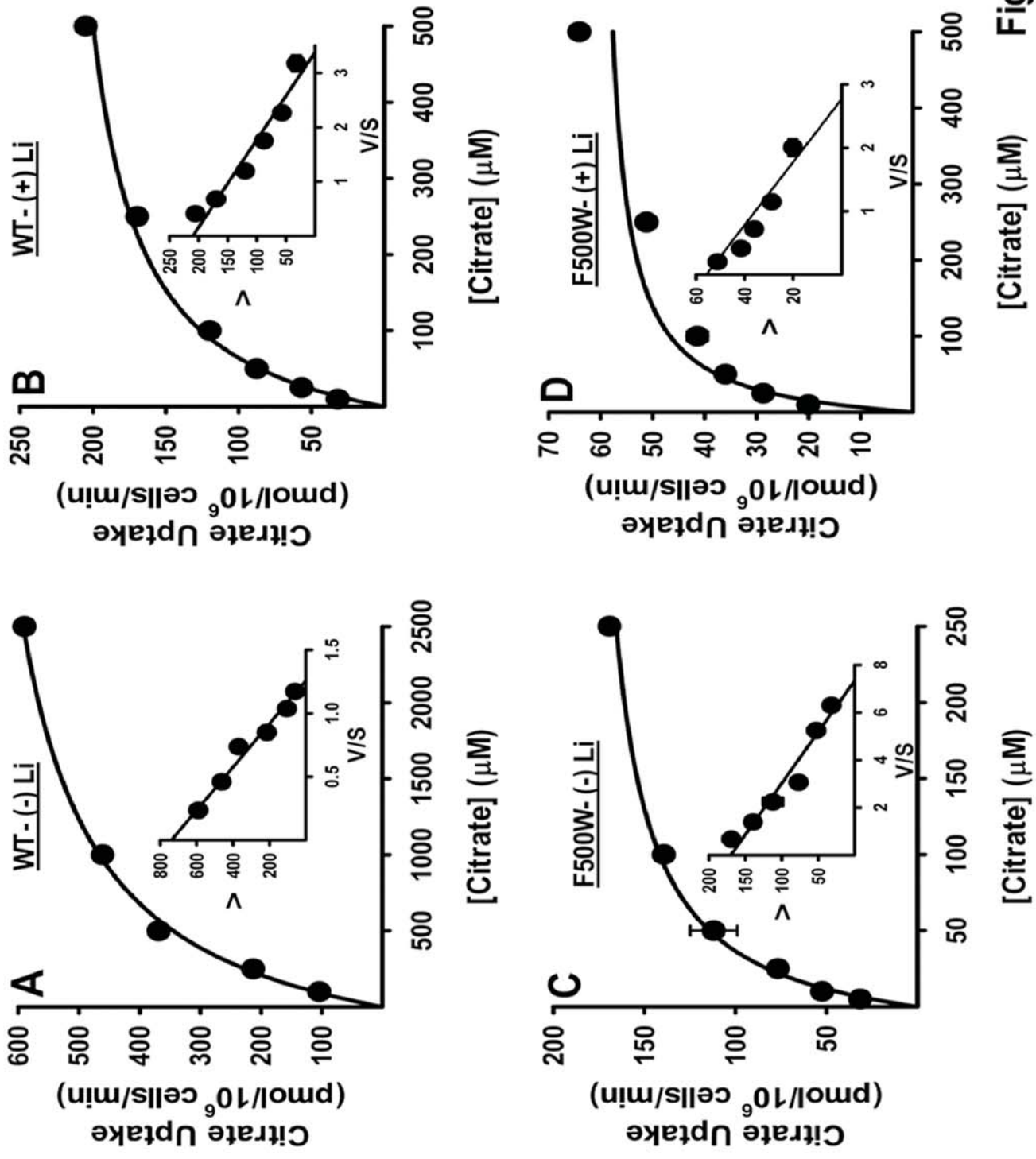

Fig. 7

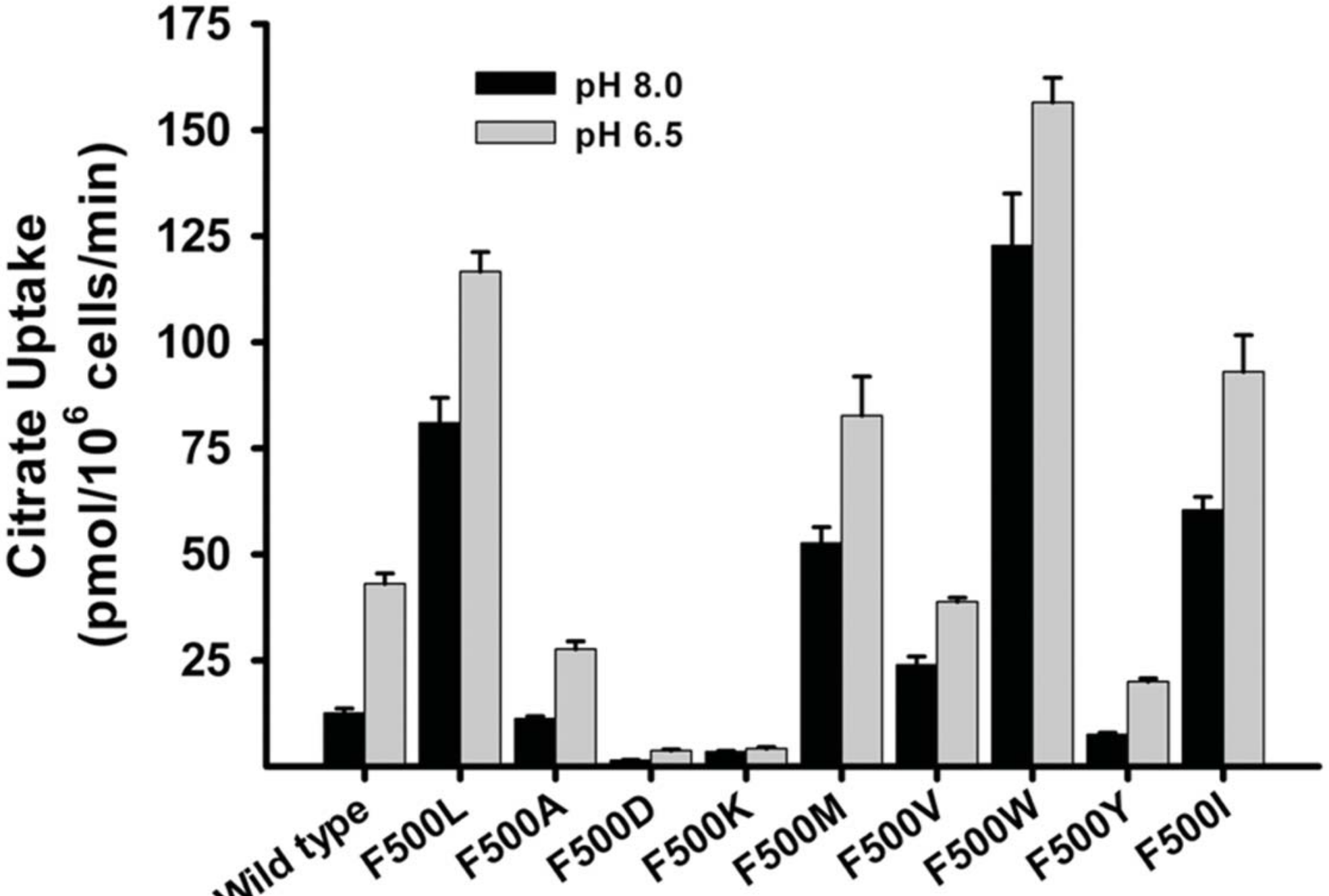

Fig. 8

JPET Fast Forward. Published on January 23, 2015 as DOI: 10.1124/jpet.114.221523
This article has not been copyedited and formatted. The final version may differ from this version.

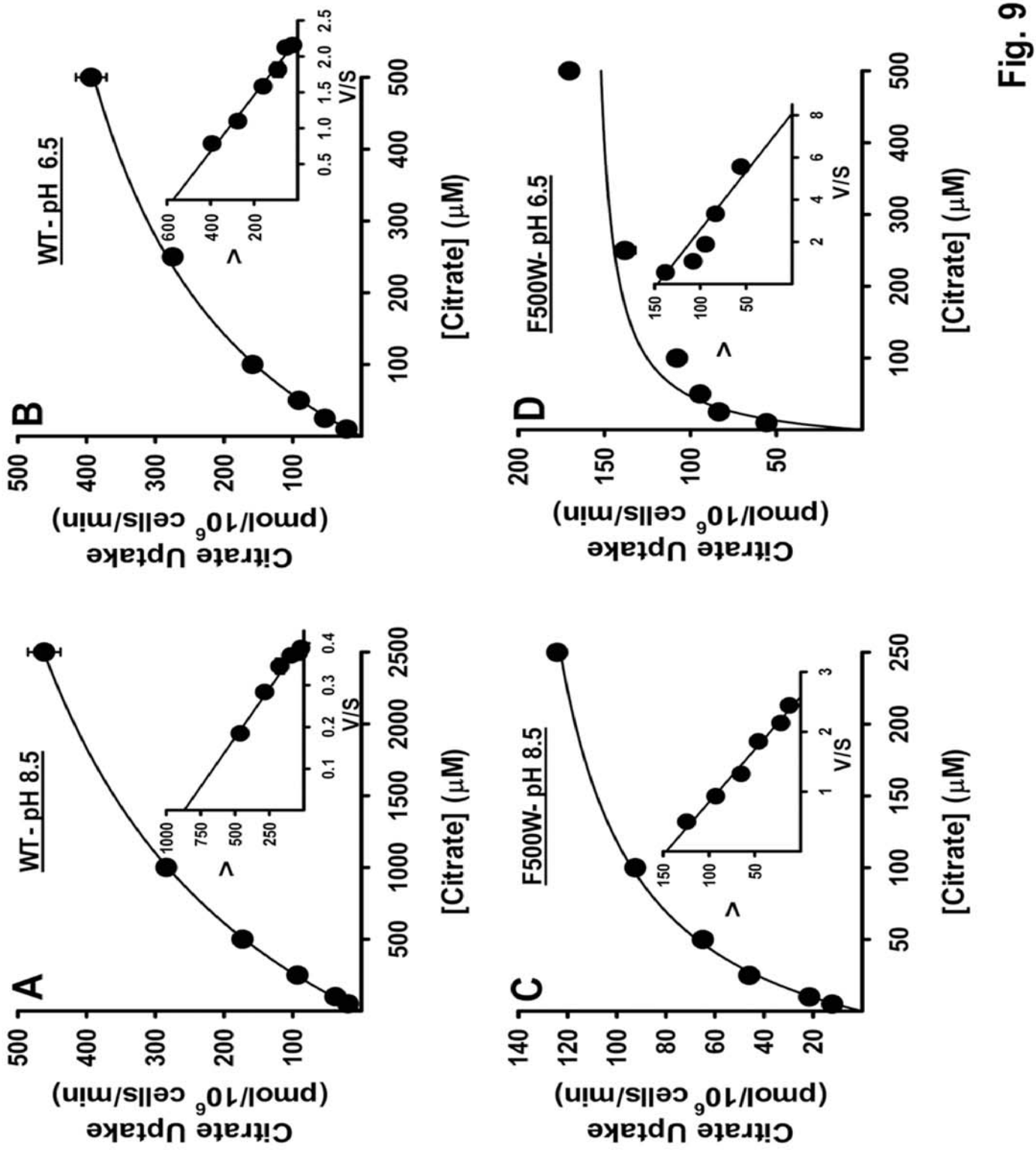

Fig. 9